International Journal of Nanoelectronics and Materials
Volume 11 (Special Issue) Dec 2018 [103-108]

Optical Investigations of Nano Lithium Niobate Deposited by Spray Pyrolysis Technique with Injection of Li_2CO_3 and Nb_2O_5 as Raw Materials

Makram A. Fakhri[1,2*], Ahmed W. Abdulwahhab[1], Marwa .A. Dawood[3], Alaa Q. Raheema[4], Najwan H. Numan[1], Farah G. Khalid[5], M. H. A. Wahid[6], U. Hashim[2] and Evan T. Salim[7]

[1]*Laser and Optoelectronic Department, University of Technology, 10066 Baghdad, Iraq.*
[2]*Institute of Nano Electronic Engineering, University Malaysia Perlis, 01000 Kangar, Perlis, Malaysia.*
[3]*Al-lsra'a University College Computer Techniques Engineering.*
[4]*Ministry of Higher Education, Baghdad, Iraq.*
[5]*Semiconductor Photonics & Integrated Lightwave Systems (SPILS), School of Microelectronic. Engineering,University Malaysia Perlis, 02600 Arau, Perlis, Malaysia.*
[6]*Collage of Agriculture, University of Baghdad, Iraq.*
[7]*Laser Science Branch, University of Technology, 10066 Baghdad, Iraq.*

ABSTRACT

In this manuscript, the physical properties of lithium-niobate films prepared by spray pyrolysis method were deeply studied. The deposition process has been taken over a quartz substrate with employing new raw materials as precursor compounds. Different annealing temperatures were applied during the deposition process. The optical results further analyzed by ultraviolet-visible (UV-Visible) and PL. The results showed that films orientation has energy band gap was measured of 3.9 eV with transmission efficiency ranges between 43 to 78%.

Keywords: Lithium Niobate, Optical Properties, Spray Pyrolysis, Optical Band Gap.

1. INTRODUCTION

Photonic Crystals (PCs) are inhomogeneous materials with spatial periodic properties. They are classified as artificial dielectric with periodically distributed structure by dielectric constant. Based on the number of dimensions [1], they have a unique band structure suitable for electromagnetic (EM) wave applications [2]. Lithium niobate ($LiNbO_3$) is one of the most popular hexagonally structured photonic materials with highly superior properties suitable for numbers of applications [3]. It shows outstanding physical and chemical properties such as high electro-optical, ferroelectrics and pyroelectrics behaviours [4,5]. The lattice parameters of the material are a = 0.5147 nm and c = 1.3862 nm [6]. Excellent optical quality single crystals lithium-niobate is widely available in markets of crystals, corresponding crystal configured has a very broad range of the Lithium/Niobieom (Li/Nb) ratio (normally from 0.9 to 1.0) [7, 8]. Different approaches were used to synthesize undoped $LiNbO_3$ nanocrystals such as sol–gel method [9, 10], soft-chemistry [11], pulsed laser deposition (PLD) [12] hydrothermal methods [13], thermal plasma spray chemical vapor deposition [14], and spray pyrolysis techniques [15].

In this work, the physical and optical properties of the prepared lithium-niobate by spray pyrolysis deposition technique were testes and discussed in details. The deposition process of the material was performed on a quartz substrate. The chosen of quartz substrate was to ensure high compatibility of the host material during processing technique. The deposition technique of

* Corresponding Author: *mokaram_76@yahoo.com*

spray pyrolysis was chosen to prepare the nano samples of lithium-niobate from raw materials of Lithium carbonate (Li_2CO_3) and niobium oxide (Nb_2O_5). In this paper, the technique used was not exposed in any literature up to recent.

2. EXPERIMENTAL

The raw materials used to prepare lithium-niobate films were lithium carbonate (Li_2CO_3) and niobium oxide (Nb_2O_5). The preparation process of Li-Nb was performed by mixing raw materials with byethylene glycol and citric acid in one solution. This process has been maintained with a continuous heating and stirring at 90°C for 48 hours. The sol is then immediately atomized (sprayed) and heated up to 400°C over a wafer of borosilicate quartz substrate. By the means of solid state reaction between Nb_2O_5 and Li_2CO_3 the lithium-niobate particles were produced as summarized in the following chemical reaction [16],

$$Nb_2O_5 + Li_2CO_3 \longrightarrow 2LiNbO_3 + CO_2 \quad (1)$$

According to (1), the air pressure and spraying distance were 2 N/m2 and 28 cm, respectively. The resultant samples were had a very smooth surface, brownish and highly adhesive properties. To ensure complete removal of organics substances, all samples were calcined in oxygen atmosphere at three annealing temperatures of 400, 500 and 600°C for at least 2 hours.

At room temperature, a spectroscopy (JobinYvon model HR 800 UV system, Kyoto, Japan) was used to examine the photoluminescence properties using He-Cd laser (λ=352 nm). For further details about the samples optical properties, a double-beam Ultra-Violet (UV-vis) spectrophotometer (Shimadzu UV-Vis 1800, Japan) was used to support the paper results.

All other constants and coefficients such as reflectance, absorption coefficient, energy bandgap, excitation coefficient and refractive index were calculated based on measuring of transmittance and absorbance spectrum in the wavelength range 300 nm to 1100 nm. Equation (2) was used to calculate the energy of incident photon, E=hν (eV) as a function of wavelength [17-21]:

$$Eg = 1240/\lambda \quad (2)$$

The Tauc equation given in (3) was used to show the energy dependence of the absorption coefficient (α) near the band edge for band to band and excitation transition [22-24]:

$$(ah\nu) = B\,(h\nu - Eg)r \quad (3)$$

where B is a constant that is inversely proportional to the amorphousity, r is a based material number that may take different values. The interception between (α hν)1/r and (hν) at (α hν)1/r=0 gives value of the bandgap. In order to calculate the absorption coefficient is given in equation (4) [24-26]:

$$\alpha = 2.303\,(A/t) \quad (4)$$

where t is the sample thickness and A is the absorption.

3. RESULTS AND DISCUSSION

In this part of this research, the photoluminescence spectra of the prepared $LiNbO_3$ were discussed and presented in Figure 1. Different annealing are indicated different emission bands

of 340, 330, 312 and 320 nm, respectively. Energy bandgaps of 3.643, 3.757, 3.875, and 3.968 eV are corresponds to those energy bands. It was found that the most emission peak was 312nm which has an energy bandgap of 3.96 eV compared to others as shown in table 1.

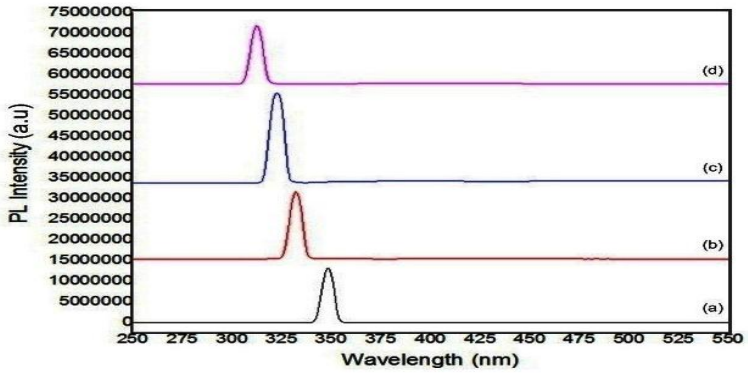

Figure 1.PL spectra of $LiNbO_3$ nanostructures for different annealing temperature (a) room temperature, (b) 400 ^oC, (c) 500 ^oC and (d) 600 ^oC.

Moreover, the relative recombination efficiency is the main factor that determines the relative peak intensity. It can be seen that the PL properties increased as the temperature starts to become higher. This increasing in the PL intensity is back to the reason of enhancement in the prepared samples structure which indicates an ideal formation of the energy bandgap compared to other bulk materials [27, 28]. As we mentioned earlier, the efficiency of radiative recombination plays a role in changing the relative peak intensity of the PL spectra. Hence, the improvement in the PL spectra facilitates that materials to be used in fabrication of photonic and optoelectronic devices. As the grains size becomes smaller and smaller, a blue shift began to appear. This is because that smaller grains behaves like a quantum wells, where the smaller grain size indicates the grain is made of only finite number of atoms, the number of overlapping orbital's or energy levels decreases and the width of the band starts to narrow, this leads to increasing bandgap as grain size decreases.

Figure 2(a) shows the transmission spectra of $LiNbO_3$ nanostructures at different annealing temperature. As it can be seen, the average optical transmission in visible light region increased with increasing annealing temperature. The reason for such increase was because of increasing structure homogeneity, thickness reduction of the film, and the thermal annealing process which in turns led to re-arranging the crystal. Higher optical transmission of nano LiNbO3 deposit was obtained at 600 °C as given in Table 1. This result attributed to higher crystallization, as well as decrement in film thicknesses, because of the film thickness inversely proportional to the transmission according to Eq. (4). The reduction of film thicknesses is consistent with the results of other studies [29-31]. The values of transmission increased from about 43% to 78% at higher annealing temperatures (room temperature up to the 600 °C). The deposited samples without annealed were at the highest thickness to produce the lowest transmittance, which is due to excessive $LiNbO_3$ atoms in the structure [32]. The low value of transmittance is attributed to the excessive $LiNbO_3$ ions, existing at interstitial sites, which probably absorbs the light. Meanwhile, high annealing temperature leads to diminution of film thickness and then enhancing the transmittance value. According to the absorption coefficient spectra, Figure 2(b) shows prepared $LiNbO_3$ nanostructures over the wavelength range 300–800 nm at room temperature. It can be noticed that this value is gradually decreased as the annealing temperature increased. This reduction in absorption value is due to the reduction in the value of samples thicknesses. The absorption coefficient's value was initially high at shorter wavelengths, but it began to sharply decline with as the wavelength increasing within the region closed to energy gap (Eg).

The estimated value of the energy bandgap found from the plot (αhv) 2 vs. (hν) (Figure 2c. and Table 1) accepted with the results mentioned in other works referenced by references [33,34]. The double-beam UV-vis was used to use to measure the optical reflectance (R%) of $LiNbO_3$ nanostructures. Further, It was calculated using the absorption and transmittance spectrum through the relation; R+T+A = 1. Figure 3d shows the reflectance of $LiNbO_3$ nanostructures in the wavelength range of 300-800 nm at room temperature. It was observed that the reflection increased with annealed temperature due to reduction of film thickness, hence transmission decreased.

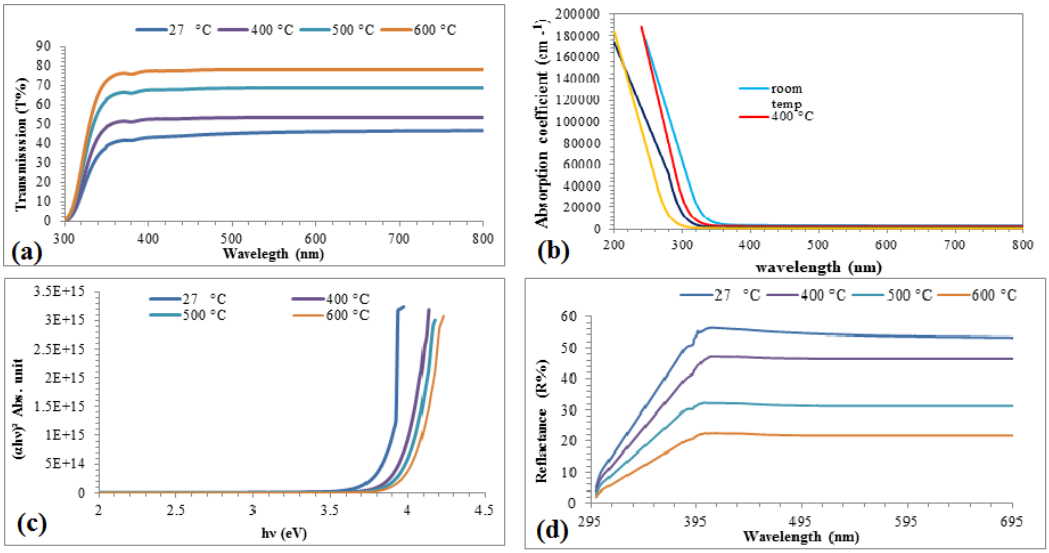

Figure 2. Prepared samples of lithium-niobate nanoparticles at different annealing temperatures (a) the transmission spectra, (b) absorption coefficient, (d) energy bandgap and (d) the reflection spectra.

Table 1 The energy band gap, refractive index and optical dielectric constant of $LiNbO_3$ annealed at different temperatures

Annealing Temp	E_g (eV) UV	E_g (eV) PL	E_g (eV) exp [33-35]	T (%)
room temp	3.78	3.643	2.66- 4.22	43.58
400	3.83	3.757		53.29
500	3.87	3.875		68.61
600	3.96	3.968		78.08

Figure 3 shows thickness dependability with annealed temperature, which leads to an increment to films homogeneity. These results are consistent with those of previous reports [35, 36].

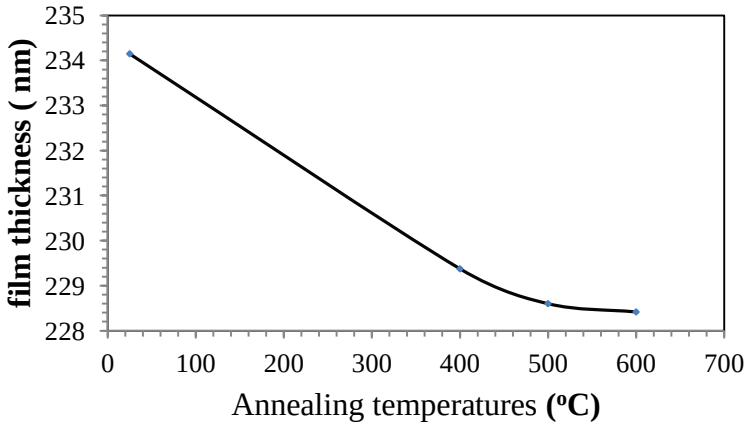

Figure 3. Thickness of $LiNbO_3$ nanostructures for different annealing temperatures.

4. CONCLUSION

$LiNbO_3$ nanostructures were chemically prepared by the spray pyrolysis technique. The grain size of the prepared crystal decreased with increment of annealing temperatures. Energy band gap was observed and measured via UV-v is and PL. The maximum transmission was found approximately 78%. Refractive index showed the highest value of 2.42, whereas 2.43 that is appropriate for optical waveguide. Optical conductivity increased from 1.8 × 104 to 2.4 × 104 (sec-1). The real and imaginary parts of dielectric constant (ε_r, ε_i) and Urbach energy were decreased as annealing temperature increased.

REFERENCES

[1] Makram A Fakhri, Evan T Salim, Ahmed W Abdulwahhab, U Hashim, Zaid T Salim, Optics Laser Technology. **103** (2018) 226-232.
[2] P. S. Bullena, H.-C. Huangb, H. Yangb, J. I. Dadapb, I. Kymissisb, RM. Osgood Jr, Optical Materials. **57** (2016) 243.
[3] Zaid T Salim, U Hashim, MK Md Arshad, Makram A Fakhri, Evan T Salim, Materials Research Bulletin. **86** (2017) 215-219.
[4] V. Bornand, I. Huet, Materials chemistry and Physics. **77** (2003) 571.
[5] E. Dogheche, X. Lansiaux, D. Remiens, J. Appl. Phys. **93** (2003) 1165.
[6] M. A. Fakhri, Y. Al-Douri, U. Hashim, E. T. Salim, Advanced Materials Research. **1133** (2016) 457-461.
[7] M. Liu, D. A. Xue, Materials Letters. **59** (2005) 2908.
[8] Zaid T Salim, U Hashim, MK Md Arshad, Makram A Fakhri, Evan T Salim, Microelectronic Engineering. 179 (2017) 83-90.
[9] K. Peithmann, M. Zamani-Meymian, M. Haaks, K. Maier, B. Andreas, K. Bbuse, Appl. Phys. B **82** (2006) 419.
[10] Zaid T Salim, U Hashim, MK Md Arshad, Makram A Fakhri, Int. J. Appl. Eng. Res **11** (2016) 8785-8790.
[11] M. Nyman, T. M. Anderson, P. P. Provencio, Cryst. Growth Des **9** (2009) 1036.
[12] X. Wang, Y. Liang, S. Tian, W. Man, J. Jia, Journal of Crystal Growth **375** (2013) 73.
[13] G. Isobe, P. Bornmann, T. Hemsel, T. Morita, Proceedings of Symposium on Ultrasonic Electronics **32** (2011) 19.
[14] Makram A. Fakhri, Evan T. Salim, M. H. A. Wahid, U. Hashim, Zaid T. Salim, Journal of Materials Science: Materials in Electronics **29**, 11 (2018) 9200-9208.
[15] V. Bornand, I. Huet, Ph. Papet, Materials Chemistry and Physics **77** (2002) 571.

[16] M. A. Fakhri, U. Hashim, E. T. Salim, Zaid T. Salim, Journal of Materials Science: Materials in Electronics **27**, 12 (2016) 13105-13112.
[17] M. A. Fakhri, E. T. Salim, U. Hashim, A. W Abdulwahhab, Z. T Salim, Journal of Materials Science: Materials in Electronics **28** (2017) 16728-16735.
[18] E. T. Salem, Makram A. Fakhry, Hala Hassen, Int. J. Nanoelectronics and Materials **6**, 2 (2013) 121-128.
[19] E. T. Salim, Raid A. Ismail, Makram A. Fakhry, Yushamdan Yusof, Int. J. Nanoelectronics and Materials **9** (2016) 111-122.
[20] Makram. A. Fakhri , F. Hattab, Engineering Sciences (FNCES), 2012 First National Conference, IEEE, (2012) 1-5.
[21] M. Caglar, S. Ilican, Y. Caglar, F. Yakuphanoglu, Applied Surface Science **255** (2009) 4491.
[22] Makram A Fakhri, Evan T Salim, M.H.A. Wahid, U Hashim, Zaid T Salim, Raid A Ismail, Journal of Materials Science: Materials in Electronics **28** (2017) 11813-11822.
[23] A. S. Hassanien, A. A. Alaa. Journal of Alloys and Compounds **648** (2015) 280.
[24] A. S. Hassanien, A. A. Alaa. Superlattices and Microstructures **89** (2016) 153.
[25] M. Steve M. Young, Fan Zheng, Andrew M. Rappe, Phys. Rev. Appl. **4** (2015) 054004.
[26] C. Thierfelder, S. Sanna, Arno Schindlmayr, W. G. Schmidt, Phys. status solidi C **7** (2010) 362.
[27] S. Shandilya, A. Sharma, M. Tomar, V. Gupta, Thin Solid Films **520** (2012) 2142.
[28] K. C. Lalithambika, K. Shanthakumari & S. Sriram, International Journal of ChemTech Research **6** (2014) 3071.
[29] M. D. Femi, A. Ohwofosirai, A. Sunday, O. S. B. A. E. F. I. Ezema, R. U. Osuji, International Journal of Advances in Electrical and Electronics Engineering **2** (2014) 331.
[30] I-S. Bae & S-J.Cho, Thin Solid Films **516** (2008) 3577.
[31] P. Li-Ping, F. Liang, W. Wei-Dong, W. Xue-Min & L. Li, Chin. Phys. B **21** (2012) 047305.
[32] Makram A Fakhri, Int. J. Nanoelectronics and Materials **9** (2016)93-102.
[33] S. Hwang, J. Lee, C. Jeongb & Y. Jooa, ScriptaMaterialia **56** (2007) 17.
[34] Mosha H. Zhao, Dawn A. Bonnell, John M. Vohs, J. Vac. Sci. Technol. A **27** (2009) 1337.
[35] M. A. Fakhri, Y. Al-Douri , E. T. Salim, U. Hashim, Y. Yusof, E. B. Choo, Z. T.Salim, Y. N. Jurn, ARPN Journal of Engineering and Applied Sciences **11** (2016) 4974-4978.
[36] I. R. Agool, E. T. Salem & M. A. Hassan, International Journal of Modern Physics B **25** (2011) 1081-1089.